Biochemical and Biophysical Research Communications 433 (2013) 547–551

Contents lists available at SciVerse ScienceDirect

Biochemical and Biophysical Research Communications

journal homepage: www.elsevier.com/locate/ybbrc

^{1}H NMR-based spectroscopy detects metabolic alterations in serum of patients with early-stage ulcerative colitis

Ying Zhang [a], Lianjie Lin [a], Yanbin Xu [b], Yan Lin [a], Yu Jin [a], Changqing Zheng [a,*]

[a] Second Department of Gastroenterology, Shengjing Hospital, China Medical University, Shenyang 110004, People's Republic of China
[b] Wanlei Life Sciences (Shenyang) Co., Ltd., Shenyang 110179, People's Republic of China

ARTICLE INFO

Article history:
Received 20 February 2013
Available online 16 March 2013

Keywords:
Ulcerative colitis
NMR
Metabolomics
Serum

ABSTRACT

Ulcerative colitis (UC) has seriously impaired the health of citizens. Accurate diagnosis of UC at an early stage is crucial to improve the efficiency of treatment and prognosis. In this study, proton nuclear magnetic resonance (^{1}H NMR)-based metabolomic analysis was performed on serum samples collected from active UC patients (n = 20) and healthy controls (n = 19), respectively. The obtained spectral profiles were subjected to multivariate data analysis. Our results showed that consistent metabolic alterations were present between the two groups. Compared to healthy controls, UC patients displayed increased 3-hydroxybutyrate, β-glucose, α-glucose, and phenylalanine, but decreased lipid in serum. These findings highlight the possibilities of NMR-based metabolomics as a non-invasive diagnostic tool for UC.

1. Introduction

Ulcerative colitis (UC), one of the two variations of inflammatory bowel diseases (IBDs), is characterized by chronic and relapsing inflammation of the large intestine [1,2]. Despite sharing similar symptoms, UC is distinct from Crohn's disease (CD) which belongs to another form of IBDs. Due to the high prevalence in the population, UC increasingly becomes a huge burden for patients and society [3–5]. It has been generally accepted that UC is a multifactorial disease which involved hereditary, environmental and microbiological factors and abnormal immune responses [6–8]. Nevertheless, the exact pathogenesis of UC still remains to be fully elucidated. Currently, the diagnostic methods for UC include endoscopic, radiologic and histological techniques [9,10]. However, all of these are time-consuming and invasive methods. Consequently, it is urgent to develop novel minimally invasive methods for accurate and early diagnosis of UC.

Nuclear magnetic resonance (NMR) spectroscopy based metabolic profiling of biofluids, such as serum and urine, has been widely used in characterizing potential biomarkers in a variety of diseases [11–13]. This approach requires only small amounts of sample to generate metabolic profiles. More importantly, it is a non-invasive method. Recently, several groups have reported the application of NMR spectroscopy based metabolomic analysis in IBDs research. NMR-based metabolic profiling of urine [14,15] and fecal extracts [9,16] has been successfully used in discriminating IBD patients from healthy subjects. Moreover, it has been demonstrated that this approach could also be used in a mouse model of UC [17]. However, metabolic profiling of serum is relatively rare. One study has investigated serum metabolic profiles of IBD patients using gas chromatography/mass spectrometry (GC/MS). Unfortunately, this study did not restrict recruitment to active IBD patients [18]. More recently, Schicho et al. have reported that NMR-based metabolic profiling of serum, plasma, and urine discriminates between patients with IBD and healthy individuals [19]. However, these samples were collected from patients with long disease duration (5.5 years). Thus, the obtained results may not reflect metabolic changes in the early stages of UC. Additionally, due to the gender imbalance in sample recruitment, the influence of gender on metabolic profiles cannot be totally ruled out.

In the current study, we used high-resolution ^{1}H NMR-based metabolic profiling of serum to determine metabolic alterations between UC patients and healthy controls. We recruited active UC patients with short disease duration (2.7 years) and minimized gender imbalance by enrolling a substantially balanced number of male and female subjects in our present study. The main objective of this study was to determine whether NMR-based metabolomics could be used as an effective non-invasive method for early stage diagnosis of UC.

2. Materials and methods

2.1. Subjects

All subjects were recruited from Shengjing Hospital of China Medical University. This study was approved by the Ethics

* Corresponding author. Address: Second Department of Gastroenterology, Shengjing Hospital, China Medical University, 36 Sanhao Street, Shenyang 110004, People's Republic of China.
E-mail address: changqing_zheng@126.com (C. Zheng).

0006-291X/$ - see front matter © 2013 Elsevier Inc. All rights reserved.
http://dx.doi.org/10.1016/j.bbrc.2013.03.012

Table 1
Characteristics of UC patients and healthy controls.[a]

	UC	Controls
No. of subjects	20	19
Gender (male/female)	9/11	9/10
Age, years, (mean, range)	42 (22–62)	37 (22–58)
Age at diagnosis (<37 years/>37 years)	9/11	–
Years with disease (⩽2 years/>2 years)	11/9	–
Disease duration, years (mean, range)	2.7 (0.08–10)	–
Mayo-score (mean, range)	8.6 (5–12)	–
Inflammation (P/PS/LC/PC)	6/6/1/7	–
Extra intestinal manifestations (present/never present)	1/19	–
Medications		
Gentamicin	20	–
Mesalamine	19	–
Methylprednisolone	2	–
Dexamethasone	17	–
Xilei-san	18	–
Kangfuxing	1	–
Hemocoagulase	9	–

[a] P, proctitis; PS, proctosigmoiditis; LC, left-sided colitis; PC, pancolitis. Extra intestinal manifestations from skin, eyes, liver and/or joints: present/never present.

Committee of China Medical University, and written informed consent was obtained from each participant. Serum samples were collected from active UC patients ($n = 20$) and healthy controls ($n = 19$), respectively. Each patient had been diagnosed with UC according to well-established criteria on the basis of clinical, histological and endoscopic techniques. Patients with quiescent UC, severe mental illness, age over 75 years or below 18 years, clinical evidence of active infections, were eliminated from this study. Additionally, patients who were pregnant or taking antibiotics recently (within two weeks) were also excluded. The characteristics of all subjects are summarized in Table 1.

2.2. Sample collection and preparation

To minimize dietary influence, serum samples were obtained from all subjects after overnight fasting. Blood samples were collected from each participant into tubes with sodium-heparin. Centrifugation was performed at 12,000 rpm, 4 °C, for 15 min. Approximately 1 mL supernatant was obtained and stored at −80 °C. At the time of NMR analysis, serum samples were thawed at room temperature. After centrifugation, 100 μL D_2O was added to 400 μL supernatant to provide a field frequency lock. Subsequently, the homogenized mixture was transferred to a 5 mm NMR tube.

2.3. NMR measurements

All ^{1}H NMR spectra were acquired on a Varian Inova 600 MHz spectrometer (Varian Inc., Palo Alto, CA, USA) operating at 599.93 MHz for ^{1}H observation and equipped with a CryoProbe at 298 K. In this study, Carr–Purcell–Meiboom–Gill (CPMG) ^{1}H NMR spectra were acquired using the following parameters: spectral width 8000.0 Hz, relaxation delay 2.1 s, acquisition time 1.0 s, total spin-echo time 100 ms, and 128 scans.

2.4. Data processing

The obtained spectral data were phased and baseline-corrected using TopSpin software package (version 3.0, Bruker Biospin, Rheinstetten, Germany). These NMR spectra were referenced and scaled to the lactate signal at 1.33 ppm. After calibration, the spectral region of 9.5–0.5 ppm was integrated into bins with equal width of 0.004 ppm using AMIX software package (version 3.9.11, Bruker Biospin). The spectral regions corresponding to the signal of residual water and urea (6.87–4.2 ppm), and ethanol (1.23–1.10 and 3.69–3.62 ppm) were excluded. All spectra were normalized to the total spectral area prior to pattern recognition analyses.

2.5. Multivariate statistical analysis

Multivariate statistical analysis was applied to a total of 39 spectra using SIMCA-P+ software package (version 11.0, Umetrics, Umea, Sweden). Principal component analysis (PCA), partial least squares discriminant analysis (PLS-DA) and orthogonal projections to latent structures (OPLS)-DA were utilized to analyze the obtained spectral data. The first and second principal components were used for all above-mentioned analyses. After mean-centering, the unsupervised PCA was performed. Subsequently, the supervised PLS-DA was carried out using unit variance scaling approach. The quality of PLS-DA models was validated by the leave-one-out cross-validation procedure. R^2X and Q^2 parameters were used to describe the quality of these models. In addition, a 200-times permutation test was performed to further assess the validity of these PLS-DA models. Finally, OPLS-DA was employed using unit variance scaling method. The correlation coefficient loading plot was generated by Matlab7.0 software package. The significance test of the Pearson's product-moment correlation coefficient was carried out to determine metabolites with significant difference between groups. The coefficient of $|r| > 0.456$ was used as the cut-off value which was calculated based on discrimination significance at the level of p-value = 0.05 and df (degree of freedom) = 17.

3. Results

3.1. ^{1}H NMR spectroscopy of serum samples

Serum samples were obtained from active UC patients ($n = 20$) and healthy subjects ($n = 19$), respectively. Typical 600 MHz CPMG ^{1}H NMR spectra of serum from a UC patient and a healthy subject are shown in Fig. 1. The endogenous metabolites detected in the spectra consisted of various amino acids including valine, leucine, isoleucine, alanine, lysine, glutamine, histidine, tyrosine, and phenylalanine, and several short chain fatty acids, for instance, acetate and butyrate. Besides, energy metabolism related molecules such as lactate, citrate and creatine, and membrane metabolites including glycerophosphocholine and choline, were also detected in these NMR spectra. However, the high interindividual variability makes it impossible to obtain consistent comparisons between UC patients and healthy controls. Thus, multivariate statistical data analysis was applied to the NMR data in order to find out metabolic alterations between these two groups.

3.2. Multivariate data analysis of NMR spectra

To discover intrinsic clusters and outliers within the data set, the unsupervised PCA was first performed with the normalized NMR spectral data. The first and second principal components (51.9% and 21.2%, respectively) were used to generate PCA models. As shown in Fig. 2A, one serum sample from UC patients was identified as an outlier and removed for further analysis. While complete separation was not observed, a trend of discrimination between UC patients and healthy controls was indicated according to the final PCA results (Fig. 2B).

To improve the separation, the supervised PLS-DA was further carried out. Likewise, PLS-DA models were created using the first and second principal components (25.4% and 9.1%, respectively).

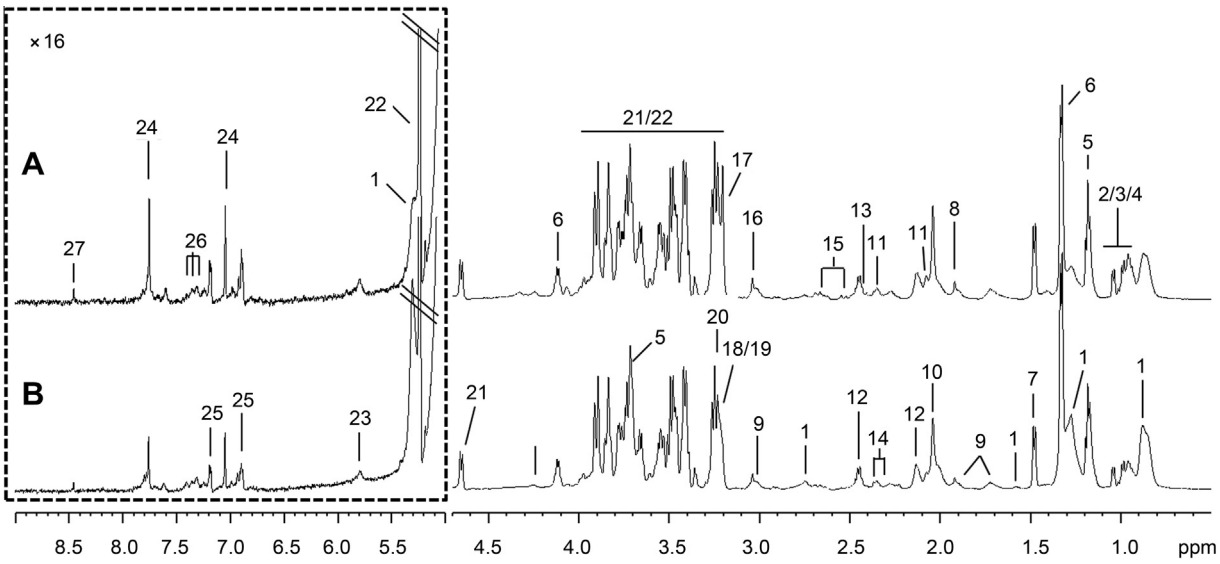

Fig. 1. Representative CPMG ^{1}H NMR spectra of serum obtained from (A) a UC patient and (B) a healthy subject. The region of δ 9.0–5.0 (in the dashed box) was magnified 16 times as compared with corresponding region of δ 4.7–0.5 for the purpose of clarity. Keys: 1, lipid; 2, valine; 3, leucine; 4, isoleucine; 5, ethanol; 6, lactate; 7, alanine; 8, acetate; 9, lysine; 10, N-acetyl-glycoprotein (NAG); 11, glutamate; 12, glutamine; 13, succinate; 14, 3-hydroxybutyrate (3-HB); 15, citrate; 16, creatine; 17, choline; 18, phosphorylcholine (PC); 19, glycerophosphocholine (GPC); 20, trimethylamine-N-oxide (TMAO); 21, β-glucose; 22, α-glucose; 23, urea; 24, histidine; 25, tyrosine; 26, phenylalanine; 27, formate.

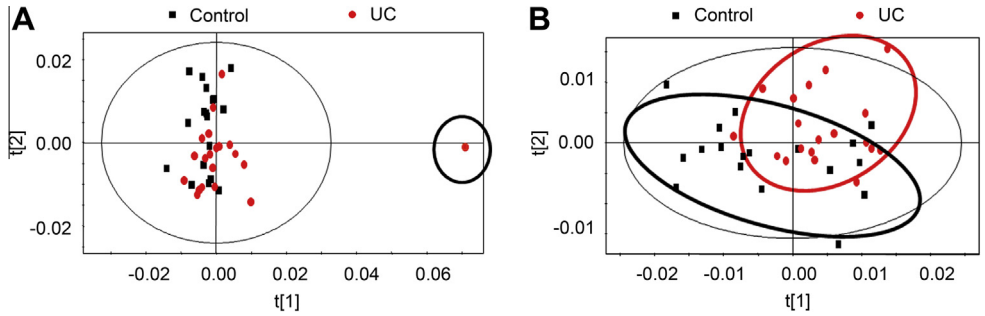

Fig. 2. PCA scores plots based on ^{1}H NMR spectra of serum obtained from UC patients and controls. (A) One serum sample from UC patients was identified as an outlier and thus removed for further analysis. (B) PCA was performed after excluding the outlier.

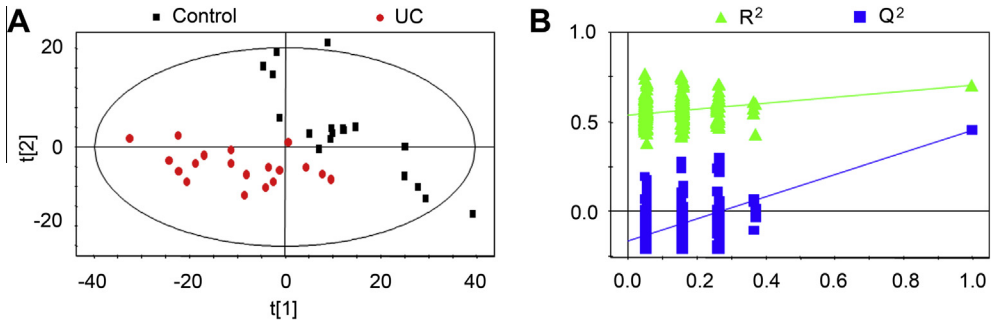

Fig. 3. PLS-DA scores plot and permutation test. (A) PLS-DA scores plot generated from ^{1}H NMR spectra of serum obtained from UC patients and controls. (B) PLS-DA models were validated by permutation test (n = 200).

The quality of these models was validated by the leave-one-out cross-validation procedure and described by R^2X and Q^2. These two parameters represent the explained variation and the predictability of the model, respectively. As shown in Fig. 3A, a good separation was achieved between patients with UC and healthy controls (R^2X = 0.32, Q^2 = 0.43). Furthermore, PLS-DA models were validated using permutation test with 200 permutations (Fig. 3B). However, these models still lack detailed information about the difference between clusters. Consequently, OPLS-DA was employed to maximize the separation and to determine the metabolic alterations between UC patients and healthy controls. A clear separation between these two groups was observed (R^2X = 0.36, Q^2 = 0.47) after OPLS-DA was performed (Fig. 4A). In addition, metabolites responsible for discriminating patients with UC from healthy controls were shown in the corresponding coefficient loading plot (Fig. 4B). Here, the direction of the peaks is associated with

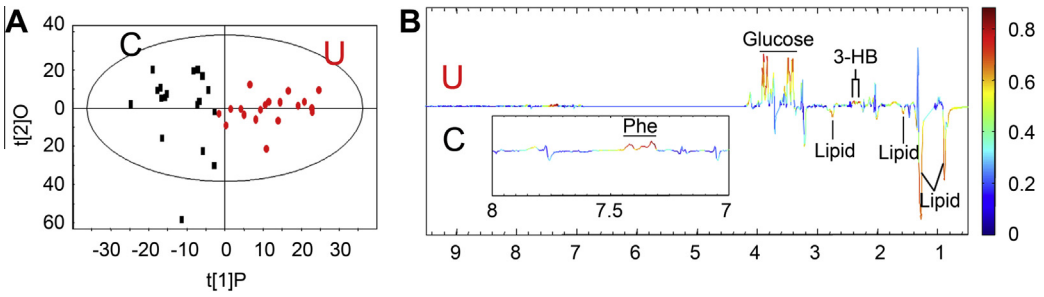

Fig. 4. OPLS-DA scores plot and corresponding coefficient loading plot. (A) OPLS-DA scores plot generated from ^{1}H NMR spectra of serum. (B) Coefficient loading plot created from OPLS-DA modeling of serum. Peaks in the positive direction denote increased metabolites in UC patients, while peaks in the negative direction indicate elevated metabolites in healthy controls. The color scaling map on the right-hand side of the coefficient loading plot represents the contribution of metabolites in discriminating UC patients from healthy controls. For key, see Fig. 1 caption. (For interpretation of the references to color in this figure legend, the reader is referred to the web version of this article.)

Table 2
OPLS-DA coefficients derived from the NMR data of metabolites in serum obtained from UC patients and healthy controls.

Metabolites	r[a] UC *vs.* control
Lipid: 0.85 (m[b]), 0.89 (m), 1.27 (m), 2.03 (m), 1.77 (m), 5.30 (m)	−0.692
3-HB: 1.20 (d), 2.31 (dd), 2.38 (dd), 4.23 (m)	0.734
β-Glucose: 3.19 (dd), 3.34 (t), 3.40 (m), 3.43 (t), 3.84 (dd), 4.48 (d)	0.636
α-Glucose: 3.36 (t), 3.47 (dd), 3.65 (t), 3.67 (m), 3.77 (m), 5.16 (d)	0.675
Phenylalanine: 7.33 (m), 7.38 (m), 7.42 (m)	0.753

[a] Correlation coefficients, positive and negative signs indicate positive and negative correlation in the concentrations, respectively. The coefficient of $|r| > 0.456$ was used as the cut-off value which was calculated based on discrimination significance at the level of p-value = 0.05 and df (degree of freedom) = 17.

[b] Multiplicity: s, singlet; d, doublet; t, triplet; q, quartet; dd, doublet of doublets; m, multiplet.

the relative concentration of specific metabolites in the cluster of interest as compared with other clusters in the established models. The color scaling map on the right-hand side of the coefficient loading plot indicates the significance of metabolites in discriminating between UC patients and healthy controls. For instance, metabolites with red color contribute more to the separation between different groups than do those with blue. The coefficients indicating the significance of metabolites contributing to the separation between these two groups are summarized in Table 2. Here, the coefficient of 0.456 was used as the cut-off value which was calculated based on discrimination significance at the level of 0.05 ($P \leqslant 0.05$). According to the loading plot, UC patients contained relatively higher serum 3-hydroxybutyrate (3-HB), β-glucose, α-glucose and phenylalanine levels than healthy controls (Fig. 4B and Table 2). In addition, lipid was decreased in UC patients as compared with healthy controls.

4. Discussion

Metabolomic profiling of biofluids, such as serum and urine, has been extensively used in characterizing potential biomarkers in a variety of diseases, including IBDs [14,15,18,20,21]. In accordance with previous findings [19], our results demonstrate that NMR-based metabolic profiling of serum can be used to discriminate between patients with active UC and healthy controls.

Regarding to the choice of biofluid, there are more studies focused on urine than those on serum in IBDs research. It has been shown that NMR-based metabolic profiling of urine samples collected from CD and UC patients and controls can be used to distinguish the cohorts [14]. Similar results have been reported in a mouse model of UC [17] or CD [22]. On the contrary, Bjerrum et al. found that the metabolic profiles of urine does not allow a differentiation between active UC, inactive UC, and controls [20]. Moreover, another group also suggested that distinguishing UC from CD via urine metabolite profile analysis may be difficult [15]. Therefore, we focused on metabolic profiling of serum samples to assess the potential application of NMR-based metabolomics in early and accurate diagnosis of UC. All serum samples were obtained after overnight fasting to avoid the potential influence of dietary factors. In regard to gender, a substantially balanced number of male and female subjects were recruited in the current study. We found that no gender-related clustering was observed based on the results of PCA. Compared to the significant metabolic alterations found in a previous report [19], we detected less marked changes in metabolite composition between UC patients and healthy controls. A possible explanation for the variations is that our results reflect metabolic changes in the early stages of UC, because serum samples obtained from UC patients with short disease duration (2.7 years) were used in the present study.

In conjunction with multivariate data analysis, we found that patients with UC displayed increased 3-HB, β-glucose, α-glucose and phenylalanine, whereas decreased lipid as compared with controls. 3-HB, a ketone body, is synthesized in the liver from acetyl coenzyme A and can be used as an energy source by the brain when blood glucose is low [23]. While higher concentration of 3-HB has been found in serum from a mouse model of UC [17], we report here that this metabolite is significantly increased in UC patients compared with healthy subjects. The strong increases of ketone bodies such as 3-HB in serum of UC patients may reflect the high demand of the body for energy. Interestingly, another group reported that 2-HB is increased in serum of IBD patients compared to controls [19]. In relation to glucose, our results further confirmed the findings described by a previous investigation [19]. Furthermore, high levels of glucose have been discovered in extracts of macroscopically uninvolved colonic mucosa of IBD patients [24]. Intriguingly, a study by Le Gall et al. found that residual glucose is somewhat higher in UC fecal extracts than in controls [16]. However, it is still not known why UC patients contain a high concentration of glucose in serum since they display malnutrition [25]. Recently, it has been shown that variations in the levels of some amino acids may be involved in the pathogenesis of IBD [26]. In contrast to the findings presented here, serum concentration of phenylalanine was not changed between UC patients and controls in a previous study [18]. Interestingly, increased phenylalanine was found in serum from a mouse model of UC [17]. Lipids can be used as stored energy and structural components of cell membranes [27]. Decreased lipids may reflect chronic and extensive

colonic inflammation associated with UC patients. Despite of the above-mentioned metabolites, it should be noted that the total number of altered metabolites is relatively low in the present study.

Acknowledgments

This study was supported by a grant from the Science and Technology Program of Liaoning Province (Grant No.: 2010225008). The funding agencies had no role in study design, data collection and analysis, decision to publish, or preparation of the manuscript.

References

[1] D.N. Frank, A.L. St Amand, R.A. Feldman, E.C. Boedeker, N. Harpaz, N.R. Pace, Molecular-phylogenetic characterization of microbial community imbalances in human inflammatory bowel diseases, Proc. Natl. Acad. Sci. USA 104 (2007) 13780–13785.
[2] E.G. Vilela, H.O. Torres, F.P. Martins, L. Ferrari Mde, M.M. Andrade, A.S. Cunha, Evaluation of inflammatory activity in Crohn's disease and ulcerative colitis, World J. Gastroenterol. 18 (2012) 872–881.
[3] Y. Wang, Q. Ouyang, Ulcerative colitis in China: retrospective analysis of 3100 hospitalized patients, J. Gastroenterol. Hepatol. 22 (2007) 1450–1455.
[4] Y.F. Wang, H. Zhang, Q. Ouyang, Clinical manifestations of inflammatory bowel disease: east and west differences, J. Dig. Dis. 8 (2007) 121–127.
[5] Y.F. Wang, Q. Ouyang, R.W. Hu, Progression of inflammatory bowel disease in China, J. Dig. Dis. 11 (2010) 76–82.
[6] S.B. Hanauer, Inflammatory bowel disease: epidemiology, pathogenesis, and therapeutic opportunities, Inflamm. Bowel Dis. 12 (Suppl 1) (2006) S3–9.
[7] W. Strober, I. Fuss, P. Mannon, The fundamental basis of inflammatory bowel disease, J. Clin. Invest. 117 (2007) 514–521.
[8] J.F. Colombel, A.J. Watson, M.F. Neurath, The 10 remaining mysteries of inflammatory bowel disease, Gut 57 (2008) 429–433.
[9] J.R. Marchesi, E. Holmes, F. Khan, S. Kochhar, P. Scanlan, F. Shanahan, I.D. Wilson, Y. Wang, Rapid and noninvasive metabonomic characterization of inflammatory bowel disease, J. Proteome Res. 6 (2007) 546–551.
[10] V. Panteris, J. Haringsma, E.J. Kuipers, Colonoscopy perforation rate, mechanisms and outcome: from diagnostic to therapeutic colonoscopy, Endoscopy 41 (2009) 941–951.
[11] E. Garcia, C. Andrews, J. Hua, H.L. Kim, D.K. Sukumaran, T. Szyperski, K. Odunsi, Diagnosis of early stage ovarian cancer by ^{1}H NMR metabonomics of serum explored by use of a microflow NMR probe, J. Proteome Res. 10 (2011) 1765–1771.
[12] N.R. Patel, M.J. McPhail, M.I. Shariff, H.C. Keun, S.D. Taylor-Robinson, Biofluid metabonomics using ^{1}H NMR spectroscopy: the road to biomarker discovery in gastroenterology and hepatology, Expert Rev. Gastroenterol. Hepatol. 6 (2012) 239–251.
[13] S. Tiziani, V. Lopes, U.L. Gunther, Early stage diagnosis of oral cancer using ^{1}H NMR-based metabolomics, Neoplasia 11 (2009) 269–276. 264p following 269.
[14] H.R. Williams, I.J. Cox, D.G. Walker, B.V. North, V.M. Patel, S.E. Marshall, D.P. Jewell, S. Ghosh, H.J. Thomas, J.P. Teare, S. Jakobovits, S. Zeki, K.I. Welsh, S.D. Taylor-Robinson, T.R. Orchard, Characterization of inflammatory bowel disease with urinary metabolic profiling, Am. J. Gastroenterol. 104 (2009) 1435–1444.
[15] N.S. Stephens, J. Siffledeen, X. Su, T.B. Murdoch, R.N. Fedorak, C.M. Slupsky, Urinary NMR metabolomic profiles discriminate inflammatory bowel disease from healthy, J. Crohns Colitis 7 (2012) e42–e48.
[16] G. Le Gall, S.O. Noor, K. Ridgway, L. Scovell, C. Jamieson, I.T. Johnson, I.J. Colquhoun, E.K. Kemsley, A. Narbad, Metabolomics of fecal extracts detects altered metabolic activity of gut microbiota in ulcerative colitis and irritable bowel syndrome, J. Proteome Res. 10 (2011) 4208–4218.
[17] R. Schicho, A. Nazyrova, R. Shaykhutdinov, G. Duggan, H.J. Vogel, M. Storr, Quantitative metabolomic profiling of serum and urine in DSS-induced ulcerative colitis of mice by ^{1}H NMR spectroscopy, J. Proteome Res. 9 (2010) 6265–6273.
[18] M. Ooi, S. Nishiumi, T. Yoshie, Y. Shiomi, M. Kohashi, K. Fukunaga, S. Nakamura, T. Matsumoto, N. Hatano, M. Shinohara, Y. Irino, T. Takenawa, T. Azuma, M. Yoshida, GC/MS-based profiling of amino acids and TCA cycle-related molecules in ulcerative colitis, Inflamm. Res. 60 (2011) 831–840.
[19] R. Schicho, R. Shaykhutdinov, J. Ngo, A. Nazyrova, C. Schneider, R. Panaccione, G.G. Kaplan, H.J. Vogel, M. Storr, Quantitative metabolomic profiling of serum, plasma, and urine by ^{1}H NMR spectroscopy discriminates between patients with inflammatory bowel disease and healthy individuals, J. Proteome Res. 11 (2012) 3344–3357.
[20] J.T. Bjerrum, O.H. Nielsen, F. Hao, H. Tang, J.K. Nicholson, Y. Wang, J. Olsen, Metabonomics in ulcerative colitis: diagnostics, biomarker identification, and insight into the pathophysiology, J. Proteome Res. 9 (2010) 954–962.
[21] H.M. Lin, N.A. Helsby, D.D. Rowan, L.R. Ferguson, Using metabolomic analysis to understand inflammatory bowel diseases, Inflamm. Bowel Dis. 17 (2011) 1021–1029.
[22] H.M. Lin, S.I. Edmunds, N.A. Helsby, L.R. Ferguson, D.D. Rowan, Nontargeted urinary metabolite profiling of a mouse model of Crohn's disease, J. Proteome Res. 8 (2009) 2045–2057.
[23] O.E. Owen, A.P. Morgan, H.G. Kemp, J.M. Sullivan, M.G. Herrera, G.F. Cahill Jr., Brain metabolism during fasting, J. Clin. Invest. 46 (1967) 1589–1595.
[24] U. Sharma, R.R. Singh, V. Ahuja, G.K. Makharia, N.R. Jagannathan, Similarity in the metabolic profile in macroscopically involved and un-involved colonic mucosa in patients with inflammatory bowel disease: an in vitro proton (^{1}H) MR spectroscopy study, Magn. Reson. Imaging 28 (2010) 1022–1029.
[25] F.C. Edwards, S.C. Truelove, The course and prognosis of ulcerative colitis, Gut 4 (1963) 299–315.
[26] Y. Shiomi, S. Nishiumi, M. Ooi, N. Hatano, M. Shinohara, T. Yoshie, Y. Kondo, K. Furumatsu, H. Shiomi, H. Kutsumi, T. Azuma, M. Yoshida, GCMS-based metabolomic study in mice with colitis induced by dextran sulfate sodium, Inflamm. Bowel Dis. 17 (2011) 2261–2274.
[27] M. Edidin, Lipids on the frontier: a century of cell-membrane bilayers, Nat. Rev. Mol. Cell Biol. 4 (2003) 414–418.